BIOCHEMISTRY
including biophysical chemistry & molecular biology

Rapid Report

pubs.acs.org/biochemistry

# Characterizing the Dynamics of the Leader−Linker Interaction in the Glycine Riboswitch with Site-Directed Spin Labeling

Jackie M. Esquiaqui,[†] Eileen M. Sherman,[‡] Sandra A. Ionescu,[†] Jing-Dong Ye,*[,‡] and Gail E. Fanucci*[,†]

[†]Department of Chemistry, University of Florida, P.O. Box 117200, Gainesville, Florida 32611, United States

[‡]Department of Chemistry, University of Central Florida, 4000 Central Florida Boulevard, Orlando, Florida 32816, United States

Supporting Information

**ABSTRACT:** Site-directed spin labeling with continuous wave electron paramagnetic resonance (EPR) spectroscopy was utilized to characterize dynamic features of the kink−turn motif formed through a leader−linker interaction in the *Vibrio cholerae* glycine riboswitch. Efficient incorporation of spin-labels into select sites within the phosphate backbone of the leader−linker region proceeded via splinted ligation of chemically synthesized spin-labeled oligonucleotides to *in vitro* transcribed larger RNA fragments. The resultant nitroxide EPR line shapes have spectral characteristics consistent with a kink−turn motif and reveal differential backbone dynamics that are modulated by the presence of magnesium, potassium, and glycine.

Riboswitches exemplify a class of RNA molecules that function to regulate genetic expression through recognition and selective binding of metabolites independent of proteins.[1,2] Binding of cognate ligands is known to modulate RNA structure and dynamics that influences the transcription, translation, or alternative splicing processes of genes associated with the bound ligands.[3,4] Regulatory ligands bind to the aptamer domains of riboswitches and induce conformational changes in the downstream expression platforms. The glycine riboswitch contains two tandem aptamers (Figure 1A), and this tandem domain resides upstream from and regulates the expression of genes associated with glycine metabolism.[5]

Recently, in-line probing experiments have shown that the leader−linker interaction increases glycine binding affinity and removes the previously accepted cooperativity between the two glycine binding sites.[6,7] Mfold analysis indicates that the leader sequence forms a conserved (>90%) P0 duplex with the linker sequence between the two aptamers.[6,8] Further analysis revealed that in ∼50% of sequences, including the *Vibrio cholerae* (VC) glycine riboswitch, the leader−linker interaction forms a commonly found RNA structural element, the kink−turn motif, which is boxed in Figure 1A.[6,9]

Here, site-directed spin labeling (SDSL) electron paramagnetic resonance (EPR) spectroscopy is used to characterize the RNA backbone dynamics of the leader−linker interaction in the VC glycine riboswitch. SDSL investigations of conformational dynamics in nucleic acids have been reported,[11−13] and within, we follow protocols of Qin for R5 spin-label attachment.[14] This chemical modification scheme is shown in Figure 1B. Although this approach is facile for smaller RNAs, when spin

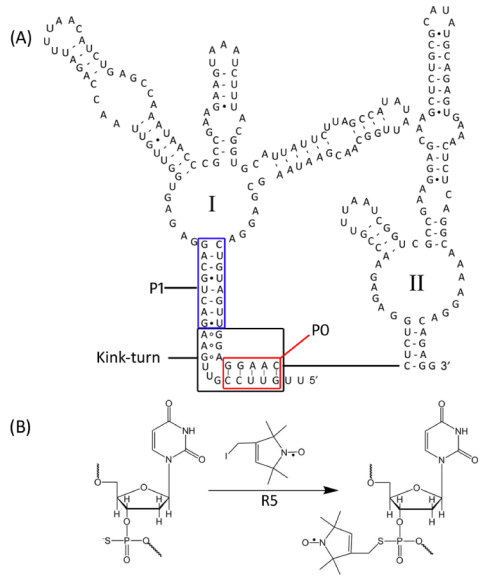


**Figure 1.** (A) Secondary structure of the 232-nucleotide VC glycine riboswitch with the kink−turn motif boxed in black, the P0 duplex boxed in red, and P1 boxed in blue.[8,10] (B) Site-directed spin labeling scheme using phosphorothioate-modified RNA and the R5 spin-label.

labeling larger constructs (>40 nucleotides), other strategies must be considered, such as using chemically synthesized spin-labeled small segments with large segments in trans,[15] or other chemical ligation means.[16]

For the VC glycine riboswitch, optimized splinted ligation using T4 DNA ligase was employed. This methodology has been used to enzymatically ligate shorter modified RNA fragments to produce large RNAs that contain desired probes or tags.[17] Here, chemically synthesized RNA oligomers that comprised the 5′ leader sequence and a site-specific phosphorothioate modification were designed. After spin labeling with R5, these oligomers were then ligated to the *in vitro* transcribed[18] remaining sequence of the VC glycine riboswitch. In our hands, optimized conditions[19] for splinted ligation with T4 DNA ligase[20] have allowed for the production of pure, full length (232 nucleotides), spin-labeled riboswitches in yields satisfactory for several EPR and biochemical control experiments. In-line probing control experiments[21,22] show that labeled riboswitches exhibit patterns

**Received:** April 3, 2014
**Revised:** May 20, 2014
**Published:** May 21, 2014

  

and glycine binding affinities similar to those of the wild-type construct (full details provided in the Supporting Information).

Three sites were chosen for spin-label attachment in this investigation, and their locations are shown in Figure 2A. Site 1 is between the first and second nucleotides at the 5′ end. Site 2 is within the interior of the leader–linker duplex (canonical stem/P0 helix). Site 3 is located within the internal loop of the kink–turn motif. The rationale for each is based upon expected differences in backbone dynamics for predicted secondary structural elements. Site 1 is expected to be most mobile as it is located at the 5′ end between two nucleotides that are not base paired. Site 2 resides within the interior of the leader–linker duplex between base-paired nucleotides; hence, it is expected to be the least mobile. Site 3 was chosen in the internal loop of the kink–turn motif where the R5 label is between nucleotides that are not base paired; however, this phosphodiester linkage may be constrained by the 60° angle between the helical axes of the canonical and noncanonical stems, and we expect site 3 to exhibit intermediate mobility.[23,24]

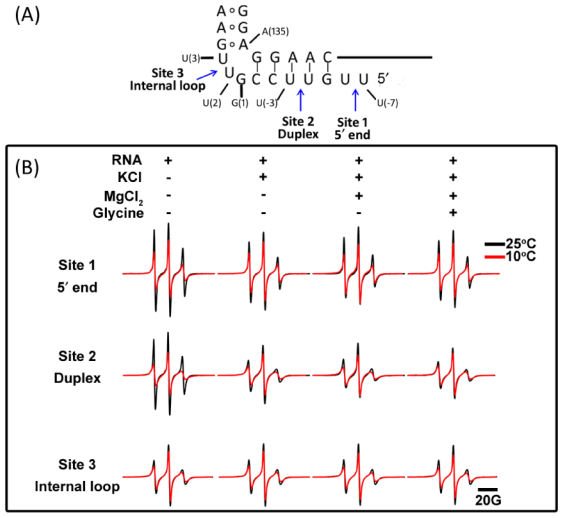


**Figure 2.** (A) Enlarged view of the leader–linker interaction with labeled sites indicated by arrows. (B) Double integral area-normalized 100 G X-band CW EPR spectra for the three sites at varying temperatures in the presence or absence of 100 mM KCl, 5 mM $MgCl_2$, and 5 mM glycine. The RNA concentration in water for each construct was approximately 100 $\mu$M.

X-Band (9.5 GHz) continuous wave (CW) EPR spectra were collected under various conditions. The influence of temperature on the dynamics of the leader–linker region was probed from spectra collected at 25 and 10 °C; these temperatures are above and below, respectively, the calculated $T_m$ value of the leader–linker duplex under physiological conditions ($T_m$ calculated using OligoCalc).[25] Glycine riboswitch folding and function are dependent upon the presence of salts and cognate glycine ligand,[26,27] and as such, data were collected for RNA alone, RNA in the presence of 100 mM KCl, RNA in the presence of 100 mM KCl and 5 mM $MgCl_2$, and RNA in the presence of 100 mM KCl, 5 mM $MgCl_2$, and 5 mM glycine.

Figure 2B shows resultant EPR spectra for the three sites under these varying conditions. CW X-band nitroxide line shapes are sensitive to changes in motion as the rotational correlation time varies between 0.1 and 50 ns.[28] Integral area-normalized spectra can be analyzed using empirical parameters such as the normalized intensity of the central-field ($h_0$) and high-field ($h_{-1}$) resonance lines (defined in Figure 3A), where larger values represent increased mobility.[29] Values of $h_0$ for each spectrum are plotted in Figure 3B.

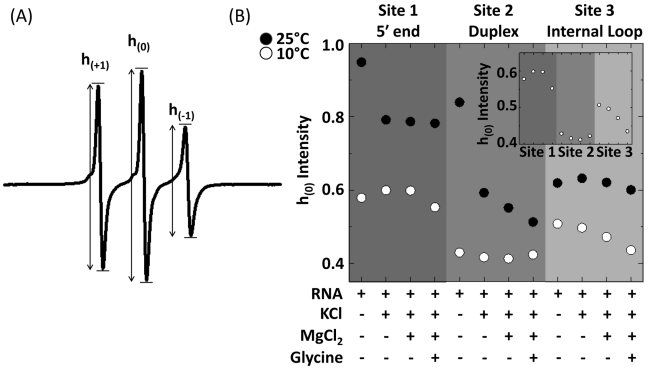


**Figure 3.** (A) Labels indicating the peak to peak intensity of the corresponding low-field, $h_{+1}$, center-field, $h_0$, and high-field, $h_{-1}$, transitions of an X-band nitroxide spectrum. (B) Plot showing the normalized intensity of $h_0$ between labeled sites at different temperatures and differing RNA folded states. Based upon triplicate measurements, the standard deviation is one-third the size of the data points.

As expected, spectra collected at 25 °C show increased mobility compared to those collected at 10 °C. In the absence of salts and glycine, the effect of temperature is more pronounced for sites 1 and 2, as would be expected, because of the increased level of motion and dynamics associated with melting of the leader–linker interaction above the $T_m$ of the duplex. Changes in dynamics upon RNA folding, induced by KCl, $MgCl_2$, or glycine, can also be observed to varying degrees for each labeled site.

For example, at 25 °C, the dynamics of site 3 are invariant, within error, upon addition of salts or glycine. For site 2, a large decrease in mobility is observed upon addition of KCl, with further decreases that could be distinguished upon addition of $MgCl_2$ and glycine ligand. In contrast, for site 1, the backbone mobility decreases upon addition of KCl only, with no further changes observed with $MgCl_2$ or glycine. The KCl-reduced mobility of sites 1 and 2 can be attributed to ionic strength-induced folding of the RNA, leading to stabilization of the leader–linker duplex. For temperatures above the $T_m$, the dynamics of the duplex are further stabilized by $MgCl_2$ and glycine, whereas for site 3, the local dynamics are less variable upon addition of KCl, which may be attributed to its proximity of the more stable P1 duplex making site 3 insensitive to the P0 dynamics.

Detailed analysis of the data collected at 10 °C, however, reveals that dynamics at site 3 are reduced upon addition of $MgCl_2$ and glycine. This agrees with a report indicating that the 60° turn is fully stabilized by $MgCl_2$.[30] In general, the overall mobility of each labeled site is in agreement with expectations of a kink–turn motif and P0 duplex formation of the leader–linker interaction, as shown with in-line probing and Mfold-predicted secondary structural motifs. The inset of Figure 3B shows that at 10 °C the 5′ end is most mobile, the duplex is least mobile, and the internal loop of the kink–turn motif exhibits intermediate motion, with sensitivity to $MgCl_2$ and glycine.

The rotation of bonds connecting the R5 spin-label to the RNA backbone is expected to influence the internal motion of R5,[28] and as expected, all spectra are in the fast limit at X-band frequency. Spectral variation, however, is still distinguishable


dx.doi.org/10.1021/bi500404b | Biochemistry 2014, 53, 3526–3528

among the three labeled sites and shows that R5 is reporting on the local environment of the RNA backbone.

Similar SDSL investigations utilizing R5 have been reported for DNA. This work extends these findings to RNA backbone dynamics.[28] Spin labeling with R5 is known to produce a diastereomerically mixed product, and previous work with DNA suggests that the combined behavior of $R_p$ and $S_p$ diastereomers can be used for general probing of the local environment.[31,32] Here, it is encouraging to see distinct spectral variation for the three labeled sites that contain R5 in both $R_p$ and $S_p$ diastereomers.

In summary, optimized splinted ligation procedures were used and allowed for efficient incorporation of the R5 spin-label into the 232-nucleotide VC glycine riboswitch for direct study of dynamics that are modulated by the folded state and ligand. X-Band SDSL is routinely utilized for characterization of conformational sampling and dynamics in proteins. Our results indicate that the R5 labeling scheme may prove to be a valuable tool for characterizing backbone dynamics in large RNAs. Specifically, this work reveals differential changes in backbone dynamics of the leader−linker region of the VC riboswitch that are modulated by salt, magnesium, and glycine.

## ■ ASSOCIATED CONTENT

### Supporting Information

Description of materials and methods, figures, and tables. This material is available free of charge via the Internet at http://pubs.acs.org.

## ■ AUTHOR INFORMATION


### Corresponding Authors

*E-mail: gefanucci@gmail.com. Phone: (352) 392-2345.
*E-mail: yejingdong@gmail.com. Phone: (407) 823-2136.



### Funding

This work was supported by National Science Foundation Grants DGE-0802270 (J.M.E.) and MCB1329467 (G.E.F.). This work was also supported by start-up funds of the University of Central Florida (J.-D.Y.) and National Institutes of Health Grants CA175625 (J.-D.Y.) and GM105409 (G.E.F.).


### Notes

The authors declare no competing financial interests.

## ■ ACKNOWLEDGMENTS


We thank Peter Qin for helpful discussions about SDSL of RNA and Yu Chen and Carol A. Fierke.


## ■ REFERENCES


(1) Serganov, A., and Patel, D. J. (2012) *Annu. Rev. Biophys. 41*, 343−370.
(2) Breaker, R. R. (2011) *Mol. Cell 43*, 867−879.
(3) Serganov, A., and Patel, D. J. (2012) *Curr. Opin. Struct. Biol. 22*, 279−286.
(4) Roth, A., and Breaker, R. R. (2009) *Annu. Rev. Biochem. 78*, 305−334.
(5) Mandal, M., Lee, M., Barrick, J. E., Weinberg, Z., Emilsson, G. M., Ruzzo, W. L., and Breaker, R. R. (2004) *Science 306*, 275−279.
(6) Sherman, E. M., Esquiaqui, J., Elsayed, G., and Ye, J. D. (2012) *RNA 18*, 496−507.
(7) Baird, N. J., and Ferre-D'Amare, A. R. (2013) *RNA 19*, 167−176.
(8) Zuker, M. (2003) *Nucleic Acids Res. 31*, 3406−3415.
(9) Kladwang, W., Chou, F. C., and Das, R. (2012) *J. Am. Chem. Soc. 134*, 1404−1407.
(10) Gardner, P. P., Daub, J., Tate, J., Moore, B. L., Osuch, I. H., Griffiths-Jones, S., Finn, R. D., Nawrocki, E. P., Kolbe, D. L., Eddy, S. R., and Bateman, A. (2011) *Nucleic Acids Res. 39*, D141−D145.
(11) Grant, G. P., Boyd, N., Herschlag, D., and Qin, P. Z. (2009) *J. Am. Chem. Soc. 131*, 3136−3137.
(12) Nguyen, P., and Qin, P. Z. (2012) *Wiley Interdiscip. Rev.: RNA 3*, 62−72.
(13) Qin, P. Z., Haworth, I. S., Cai, Q., Kusnetzow, A. K., Grant, G. P., Price, E. A., Sowa, G. Z., Popova, A., Herreros, B., and He, H. (2007) *Nat. Protoc. 2*, 2354−2365.
(14) Zhang, X., Cekan, P., Sigurdsson, S. T., and Qin, P. Z. (2009) *Methods Enzymol. 469*, 303−328.
(15) Zhang, X., Tung, C. S., Sowa, G. Z., Hatmal, M. M., Haworth, I. S., and Qin, P. Z. (2012) *J. Am. Chem. Soc. 134*, 2644−2652.
(16) Buttner, L., Seikowski, J., Wawrzyniak, K., Ochmann, A., and Hobartner, C. (2013) *Bioorg. Med. Chem. 21*, 6171−6180.
(17) Moore, M. J., and Query, C. C. (2000) *Methods Enzymol. 317*, 109−123.
(18) Sherman, E. M., Holmes, S., and Ye, J. D. (2014) *J. Mol. Biol. 426*, 2145−2157.
(19) Kurschat, W. C., Muller, J., Wombacher, R., and Helm, M. (2005) *RNA 11*, 1909−1914.
(20) Strobel, S. A., and Cech, T. R. (1995) *Science 267*, 675−679.
(21) Soukup, G. A., and Breaker, R. R. (1999) *RNA 5*, 1308−1325.
(22) Regulski, E. E., and Breaker, R. R. (2008) *Methods Mol. Biol. 419*, 53−67.
(23) Klein, D. J., Schmeing, T. M., Moore, P. B., and Steitz, T. A. (2001) *EMBO J. 20*, 4214−4221.
(24) Daldrop, P., and Lilley, D. M. (2013) *RNA 19*, 357−364.
(25) Kibbe, W. A. (2007) *Nucleic Acids Res. 35*, W43−W46.
(26) Lipfert, J., Das, R., Chu, V. B., Kudaravalli, M., Boyd, N., Herschlag, D., and Doniach, S. (2007) *J. Mol. Biol. 365*, 1393−1406.
(27) Lipfert, J., Sim, A. Y., Herschlag, D., and Doniach, S. (2010) *RNA 16*, 708−719.
(28) Popova, A. M., Kalai, T., Hideg, K., and Qin, P. Z. (2009) *Biochemistry 48*, 8540−8550.
(29) Fanucci, G. E., and Cafiso, D. S. (2006) *Curr. Opin. Struct. Biol. 16*, 644−653.
(30) Goody, T. A., Melcher, S. E., Norman, D. G., and Lilley, D. M. (2004) *RNA 10*, 254−264.
(31) Grant, G. P., Popova, A., and Qin, P. Z. (2008) *Biochem. Biophys. Res. Commun. 371*, 451−455.
(32) Popova, A. M., and Qin, P. Z. (2010) *Biophys. J. 99*, 2180−2189.